

Article

Sizing of Lithium-Ion Battery/Supercapacitor Hybrid Energy Storage System for Forklift Vehicle [†]

Théophile Paul ^{1,*} , Tedjani Mesbahi ¹ , Sylvain Durand ¹, Damien Flieller ¹ and Wilfried Uhring ²

¹ ICube Laboratory (UMR CNRS 7357) INSA Strasbourg, 67000 Strasbourg, France; tedjani.mesbahi@insa-strasbourg.fr (T.M.); sylvain.durand@insa-strasbourg.fr (S.D.); damien.flieller@insa-strasbourg.fr (D.F.)

² ICube Laboratory (UMR CNRS 7357) University of Strasbourg, 67081 Strasbourg, France; wilfried.uhring@unistra.fr

* Correspondence: theophile.paul@insa-strasbourg.fr

[†] This paper is an extended version of our paper published in 2019 IEEE Vehicular Power and Propulsion Conference, Hanoi, Vietnam, 14–17 October 2019.

Received: 17 July 2020; Accepted: 25 August 2020; Published: 1 September 2020



Abstract: Nowadays, electric vehicles are one of the main topics in the new industrial revolution, called Industry 4.0. The transport and logistic solutions based on E-mobility, such as handling machines, are increasing in factories. Thus, electric forklifts are mostly used because no greenhouse gas is emitted when operating. However, they are usually equipped with lead-acid batteries which present bad performances and long charging time. Therefore, combining high-energy density lithium-ion batteries and high-power density supercapacitors as a hybrid energy storage system results in almost optimal performances and improves battery lifespan. The suggested solution is well suited for forklifts which continuously start, stop, lift up and lower down heavy loads. This paper presents the sizing of a lithium-ion battery/supercapacitor hybrid energy storage system for a forklift vehicle, using the normalized *Verein Deutscher Ingenieure* (VDI) drive cycle. To evaluate the performance of the lithium-ion battery/supercapacitor hybrid energy storage system, different sizing simulations are carried out. The suggested solution allows us to successfully optimize the system in terms of efficiency, volume and mass, in regard to the battery, supercapacitors technology and the energy management strategy chosen.

Keywords: lithium-ion battery; supercapacitor; weight; volume; cost; hybrid electric vehicle; VDI drive cycle; forklift

1. Introduction

Industry 4.0 is part of the fourth industrial revolution [1]. With the rise of numerical technologies, sensors have become cheaper, smaller, more connected and have an increased memory storage capacity. Implemented on machines, a large amount of data can be provided and can be used to improve production lines [2]. Internet of Things (IoT), 3D printing, virtual reality, big data, artificial intelligence and collaborative robots are the main topics used to optimize the performance of “smart factories” [3–5]. Industry 4.0 is carried out by one main goal: more environmentally sustainable manufacturing, which leads to more optimal use of resources. Thereby, the use of fossil energy in factories tends to be restricted and even prohibited. One area of improvement is the use of electrical sources [1] to supply handling machines, such as forklift trucks.

Forklifts are part of the industrial environment and are useful in daily tasks when moving heavy loads from one place to another [6,7]. They have been used since the end of the 1800 s, where company

were both growing horizontally and vertically. They consist of a powertrain system used for driving and lifting operations in indoor or outdoor environments. Forklifts can be classified according to their power source: liquefied petroleum gas (LPG), diesel or electric [6,8,9]. Diesel forklifts have been mostly used because of good durability and good torque. However, for indoor applications and Industry 4.0 requirements, zero-emissions is mandatory. Therefore, electrical forklifts are widely used these past few years [10,11]. They also provide very high torque, low speed and zero noise pollution thanks to the electric motor [11]. Charging time is, however, a big concern. Batteries must be either charged for several hours or swapped if needed.

Lead-acid batteries are largely used in electric forklifts [12] due to their relatively low cost. This technology presents some downsides, such as deep discharge, which are critical to the lifespan of the battery [13]. Moreover, lead-acid batteries are heavier than lithium-ion batteries, but in forklift applications, they are used as a counterweight and help to maintain the center of gravity during operational lifts [14,15]. However, lithium-ion battery price has been decreasing [16], and this technology still presents better performances than lead-acid batteries in terms of energy density, power discharge, cycle life, efficiency, and charging operations [17,18]. Manufacturers such as Jungheinrich or EP Equipment offer forklifts equipped with lithium-ion batteries with quick charging time (2.5 h instead of 10 h with lead-acid batteries). Because of their good characteristics, less maintenance is needed with lithium-ion batteries and therefore they last much longer. Even though the price is still higher than lead-acid batteries, lithium-ion batteries present a better total cost of ownership (TCO) [19] thanks to the features previously mentioned. The counterbalance issue can be easily solved by adding ballasts within the battery to meet the battery weight specifications [12].

Moreover, forklifts repeatedly start and stop during standard operations, and therefore generate a large amount of braking power [10], which is usually converted to heat. Additionally, energy can be produced when the load is lowered down. One goal would be to recharge the battery using recovery energy during braking phases and lowering phases. However, batteries are not suitable for this kind of application: power peaks usually heat the battery and therefore decrease the battery lifetime [20,21]. As a solution here, a hybrid energy storage system (HESS) is proposed using high-energy (HE) lithium-ion batteries coupled with supercapacitors (SC).

The hybridization between a lithium-ion battery and supercapacitor was depicted as a suitable solution in terms of sizing and power performance in [22–27]. As a matter of fact, combining components with, respectively, high specific energy [17] and high specific power [28] provides an optimal electric source with assets of each energy sources [15,29,30]. Supercapacitors are then used as buffers in order to assist the battery in power [29]. Therefore, power constraints, such as high-power peaks or fast charging/discharging, are limited in the battery, which improves the overall health of the battery and extends battery life. Power from braking phases is also better recovered through supercapacitors [31,32].

In the literature [23–25,30,33–36], several sizings of lithium-ion battery supercapacitor energy storage systems for vehicles were proposed. Sizing algorithms give an estimation of the number of battery and supercapacitor cells and therefore the weight and volume of the HESS, thanks to the dynamics of the vehicle chosen. The results highly depend on the battery and supercapacitor technology but also on the energy management strategy chosen and on the driving cycle [37]. This paper is an extended version of [37]. A lithium-ion battery supercapacitor HESS sizing based on [38,39] is proposed for a forklift vehicle. The *Verein Deutscher Ingenieure* (VDI) drive cycle, suitable for this industrial application, will be presented. The remainder of the paper is organized as follows: Section 2 describes the driving cycle studied, Section 3 illustrates the principle of a lithium-ion battery/supercapacitor sizing, Section 4 presents simulation results and Section 5 offers conclusions.

2. Driving Cycles

The representation of speed versus time is called a driving cycle and it can be divided into two groups: transient driving and modal driving. The latter is composed of linear acceleration, linear

braking and constant speed phases which are not representative of a driver real behavior. NEDC drive cycle is an example of modal driving used for car consumption in Europe until 2017. On the contrary, transient driving constitutes speed variation typical of real driving conditions and driver behavior. Thus, driving cycles are built according to vehicle, environment and road conditions in order to assess the performance of an internal combustion engine (ICE) vehicle or to define the range of an electric vehicle [40]. Common driving cycles for electric vehicles from the United States (FTP-75) and Europe (ARTEMIS, NEDC) can be found in [37], as well as the Worldwide Harmonized Light Vehicles Test Procedure (WLTP).

The driving cycles previously mentioned cannot be used in this study. In fact, to assess the performance of an industrial forklift, the “*Verein Deutscher Ingenieure*” (VDI 60) drive cycle is used [9,12,41]. It consists of a cycle repeated 45 times within 60 min with a load of about 70% of the rated capacity. Details can be found in the NF ISO 16769-2 norm and are summarized as follows (Figure 1a):

- Start at position A, the forklift holds the load
- Forward travel from A to B—lift the load up to 2 m
- Lower the load and backward travel from B to C
- Forward travel from C to D—lift the load up to 2 m
- Lower the load and backward travel from D to A
- End of the cycle

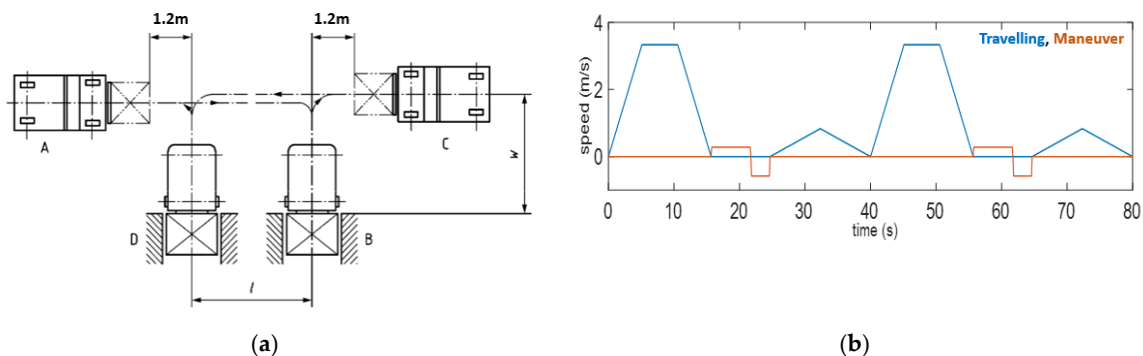


Figure 1. (a) *Verein Deutscher Ingenieure* (VDI) drive cycle protocol ($l = 30$ m and $w = 3$ m) [NF ISO 16769-2], (b) Speed profile from VDI 60 protocol (forklift: *EFG 110 Jungheinrich*)—(blue) travelling speed (orange) fork speed during handling maneuver.

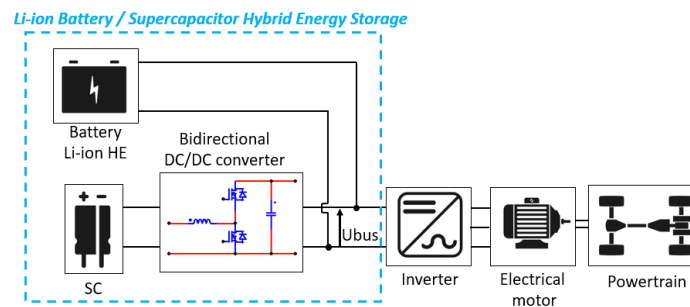
As mentioned previously, the forklift is holding a load from the beginning until the end of the cycle without dropping it. Moreover, this protocol is only suitable for electric forklifts with a rated capacity lower than or equal to 5 t and a rated battery voltage lower than or equal to 36 V. Therefore only 45 cycles should be performed within 60 min with an adapted speed both for travelling and lifting operations. Thanks to specifications from forklift manufacturers, a first approach of the cycle can be deducted and built using information such as travelling speed, load lifting and lowering speed (see Figure 1b and Table 1).

Table 1. Jungheinrich forklift dynamics.

Variable	Description	Value	SI
C_x	Drag coefficient	0.9	/
S	Forklift front surface	1.676	m^2
ρ	Air density	1.25	$kg \cdot m^{-3}$
C_1	Static rolling resistance coefficient	1.6×10^{-6}	$s^2 \cdot m^{-2}$
C_0	Dynamic rolling resistance coefficient	0.008	/
m_{fkt}	Forklift weight without battery and load	2110	kg
m_{load}	70% of maximal load weight	700	kg
g	Gravity	9.81	$m \cdot s^{-2}$
α	Angle of inclination	0	rad
/	Travelling speed with/without load	12/12.5	km/h
/	Load lifting speed with/without	0.28/0.5	m/s
/	Load lowering speed with/without	0.58/0.6	m/s

3. Methodology for Sizing Lithium-Ion Battery/Supercapacitor Hybrid Energy Storage System

There are many different architectures from passive to fully active lithium-ion battery/supercapacitor HESS [20]. The chosen topology here is a semi-active hybrid one, with a DC/DC bi-directional converter in the side of supercapacitors (Figure 2). The advantages of this configuration are mainly the reliability, better use of SC energy and a lighter overall weight compared to architectures with two DC/DC converters [15,20,29]. Moreover, the converter used allows the charge and discharge of supercapacitors and assures a lighter weight thanks to its simplicity.

**Figure 2.** Schematic of the hybrid source studied [37].

3.1. Conversion from a Driving Cycle to a Power Cycle

In order to get the power requested, dynamic equations of the forklift were established (see (1)–(3)), where V_{VEH} is the vehicle speed. The VDI cycle will define the vehicle power requirement for vehicle traction. However, handling maneuvers can be also added to the dynamic equation. In fact, some forklifts have different energy sources for travelling and lifting operation (e.g., hydraulic equipment or hybrid forklift) [8]. In our study, the electric HESS also provides power for lifting operation. Equations are detailed in ((4)–(7)). The EFG 110 forklift from Jungheinrich (Figure 3) will be used as an example, and its parameters are tabulated in Table 1.

**Figure 3.** EFG 110 from Jungheinrich.

Equations for travelling operations [38]:

$$\begin{cases} F_{aero} = 0.5 * \rho * s * C_x * V_{VEH}^2 \\ F_{wheel} = (m_{fkt} + m_{load}) * g * (C_0 + C_1 * V_{VEH}^2) \\ F_{gx} = (m_{fkt} + m_{load}) * g * \sin(\alpha) \\ F_{acc} = (m_{fkt} + m_{load}) \frac{d V_{VEH}}{dt} \end{cases} \quad (1)$$

$$F_T = F_{aero} + F_{wheel} + F_{gx} + F_{acc} \quad (2)$$

$$Pv = F_T * V_{VEH} \quad (3)$$

Equations for lifting operations:

$$F_{lift} = F_{acclift} + F_g \quad (4)$$

$$F_{acclift} = m_{load} \frac{d V_{fork}}{dt} \quad (5)$$

$$F_g = m_{load} * g * \cos(\alpha) \quad (6)$$

$$P_{lift} = F_{lift} * V_{fork} \quad (7)$$

The angle of inclination (working surface slope) is equal to zero as forklifts operate mostly on a plane surface. The load weight is equal to 70% of the maximum load, as specified in the VDI driving cycle. Friction forces were neglected in lifting operations.

3.2. Sizing of the Battery

When integrating the power cycle, the energy needed to assure the range of the vehicle is given. In our case, one VDI drive cycle corresponds to 1 h of operating time. There are three hypotheses which can lead to the battery sizing [37]:

- Ensure the maximal consuming power (using maximal power requested)
- Ensure the maximal braking power (using minimal power requested)
- Ensure only the vehicle range (using final value of the energy)

The last hypothesis will be used in order to use the battery as the main source because of its high specific energy and supercapacitors as a secondary source in regard to its high specific power. The bus voltage is set as $U_{bus} = 24 V$ (Figure 2) according to the EFG-110 specifications. The number of serial battery cells can be determined as $N_{sb} = U_{bus}/U_{elb}$ and the number of parallel battery cells, N_{pb} , thanks to Equation (15), E_{vcons} with being the energy required by the forklift for several repeated VDI drive cycles, E_{elB} representing the energy, M_{elB} the weight, R_{0elb} the internal resistance, and U_{elb} the nominal voltage for one battery cell. The depth of discharge (DOD) is the percentage of battery energy used and is limited to 80% in order to minimize the battery ageing [42], and ∂E_{vcons} is the variation of total energy according to the battery weight added to the vehicle [43]. This last variable takes into account the weight added by the battery to the vehicle. The battery is then sized in order to respect (8):

$$E_{bat} - \Delta E_V - E_{LossB} \geq E_{vcons} \quad (8)$$

with E_{bat} , the battery energy:

$$E_{bat} = N_{sb} * N_{pb} * E_{elB} * DOD \quad (9)$$

ΔE_V , the energy variation due to the added weight:

$$\Delta E_V = N_{sb} * N_{pb} * 1.4 * \partial E_{vcons} * M_{elB} \quad (10)$$

and E_{LossB} , the energetic battery loss:

$$E_{LossB} = \frac{N_{sb}}{N_{pb}} * R_{0elb} * \int_0^t I_{bat}^2 dt \tag{11}$$

$$I_{bat} = \frac{Pv + P_{lift}}{U_{bus}} \tag{12}$$

$$E_{LossB} = \frac{N_{sb}}{N_{pb}} * \frac{R_{0elb}}{U_{bus}^2} * E_L \tag{13}$$

$$E_L = \int_0^t (Pv + P_{lift})^2 dt \tag{14}$$

which leads to the following equation:

$$N_{pb} = \frac{(Ev_{cons} + \sqrt{Ev_{cons}^2 + 4(E_{elB} * DOD - \partial Ev_{cons} * 1.4 * M_{elB}) * \frac{R_{0elb}}{U_{elb}^2} * E_L})}{2 * N_{sb} * (E_{elB} * DOD - \partial Ev_{cons} * 1.4 * M_{elB})} \tag{15}$$

3.3. Energy Management Strategy

Once the battery is sized, its weight is added to the forklift and a new power requirement is calculated. This power needs to be shared into the battery (P_{bat}) and the supercapacitor (P_{sc}). Different energy managements can be used from rule-based to optimal and artificial intelligence-based algorithms [44–49]. In this study, a simple rule-based battery power limitation is used [24,50] combined with a supercapacitor energy supervision, with P_{batD} and P_{batC} being the power battery limitation block in Figure 4, respectively, the power battery limitation in discharge and in charge, as imposed by the manufacturer.

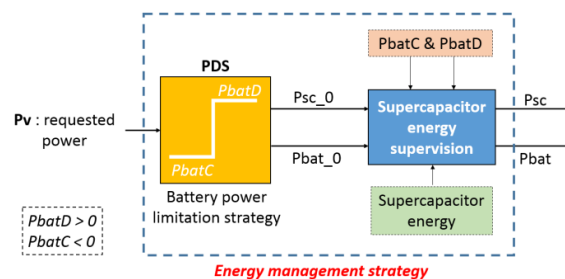


Figure 4. Energy management strategy schematic [32].

From Figure 4, Pv is split into P_{sc_0} , and P_{bat_0} , through the saturation block. In fact, power between P_{batD} and P_{batC} is sent to the battery, while power outside those limitations is sent to supercapacitors. However, supercapacitors should act like buffers that charge or discharge themselves when needed but must also be charged at a reference level at all times to provide or store energy. This means that no energy drift is allowed in the supercapacitors. To prevent this phenomenon, a supercapacitor energy supervision is implemented and redistributes the power between the battery and supercapacitor to charge or discharge the SC through the battery or the load [43]. Simulation results are given in Section 4.4.

3.4. Sizing of the Supercapacitor

Now that power sent to supercapacitors (P_{sc}) is defined, the number of serials ($N_{s_{sc}}$) and parallel ($N_{p_{sc}}$) supercapacitor cells can be found thanks to (19) and (20), with $C_{el_{sc}}$ representing the capacity, $U_{el_{sc}}$ the nominal voltage and $M_{el_{sc}}$ the weight of one supercapacitor cell. Supercapacitor energy (E_{sc}) can be obtained by integrating its power. Thus, ΔE_{sc} represents the maximal variation of E_{sc} and γ_{sc}^C and γ_{sc}^D

represent extrema of E_{sc} as a function of the weight [43,51] for charge and discharge of the supercapacitor, respectively. Here, SC losses are neglected because of their small internal resistance compared to batteries. However, although SC Columbic efficiency is high (85% to 98%), an 85% yield can be applied to calculate the worst-case energy used in a SC [52]. Then, the following equation must be respected:

$$E_{sc} \geq \Delta E_{sc} + \Delta E_{sc}^W \quad (16)$$

with ΔE_{sc}^W , which represents the variation of ΔE_{sc} according to the weight:

$$\Delta E_{sc}^W = Np_{sc} * N_{S_{sc}} * (\gamma_{sc}^C + \gamma_{sc}^D) * 1.4 * M_{el_{sc}} \quad (17)$$

E_{sc} is the energy provided by the battery pack. Only $\frac{3}{4}$ of the energy is used in one supercapacitor cell, which represents a voltage variation between nominal voltage and half the nominal voltage.

$$E_{sc} = 0.85 * \frac{3}{4} * \frac{1}{2} * Np_{sc} * N_{S_{sc}} * C_{el_{sc}} * U_{el_{sc}}^2 \quad (18)$$

These equations lead to the following final equations:

$$N_{S_{sc}} = \frac{U_{bus}}{U_{el_{sc}}} \quad (19)$$

$$Np_{sc} = \frac{\Delta E_{sc}}{\left(0.85 * \frac{3}{8} * N_{S_{sc}} * C_{el_{sc}} U_{el_{sc}}^2 - (\gamma_{sc}^C + \gamma_{sc}^D) * 1.4 * N_{S_{sc}} * M_{el_{sc}}\right)} \quad (20)$$

For battery and supercapacitor weight estimation, an additional 40% ratio [53] is added to take into account the weight of the packaging and associated electronics. See Equations (10) and (17).

3.5. DC/DC Converter Sizing

The weight of the converter can be estimated. In principle, the latter is mainly due to the weight of the self and the heat sink. In this paper, only the weight of the self is taken into account. Thus, the $Ae * Sb$ product of the self must be found and multiplied by k_1 and k_2 , respectively, for estimating the weight and the volume of the self [39], with I_{sc_max} representing the maximal current requested by the SC, I_{sc_rms} the root mean square (RMS) current, L the value of the self, B_{max} the maximal induction, J the current density, and K_B the winding ratio. The current requested by the supercapacitors is given by $I_{sc_rms} = P_{sc}/U_{bus}$ (see Table 2 and Equations (21)–(24)).

$$L = \frac{d * (1 - d) * U_{bus}}{\Delta I_{sc} * I_{sc_max} * F} \quad (21)$$

$$Ae * Sb = \frac{L * I_{sc_max} * I_{sc_rms}}{B_{max} * J * K_B} \quad (22)$$

$$Weigh_{converter} = Ae * Sb * k_1 \quad (23)$$

$$Volume_{converter} = Ae * Sb * k_1 * k_2 \quad (24)$$

Table 2. Converter data.

Variable	Description	Value
B_{max}	Maximal induction	0.4 T
J	Current density	5×10^6 A/m ²
K_B	Winding ratio	0.4
k_1	Proportionality AeSb/weight	6.54×10^6 kg·m ⁻⁴
k_2	Proportionality weight/volume	0.12 L/kg
d	Duty cycle	0.5
F	Converter frequency	15 kHz
ΔI_{sc}	Isc ripple tolerance	10%

3.6. Adjusting the Number of Cells

The final step consists of adding converter and supercapacitor weights to the dynamic model. The new power and energy requested must be calculated and should respect the following conditions:

- The energy of the battery, taking into account the DOD, is higher than the total energy requested by the vehicle range:

$$E_{bat} - E_{LossB} \geq E_{vcons} \tag{25}$$

- The supercapacitor energy, taking into account a yield of 85%, is higher than the difference between the two extrema of supercapacitor energy after energy management $E_{sc} \geq \Delta E_{sc}$.

If one of the two conditions is not respected, a parallel battery or supercapacitor branch is added respectively for the first or second condition. Then dynamics of the vehicle will be checked again until the two conditions are fulfilled. Figure 5 summarizes the algorithm described from steps 3.1 to 3.6.

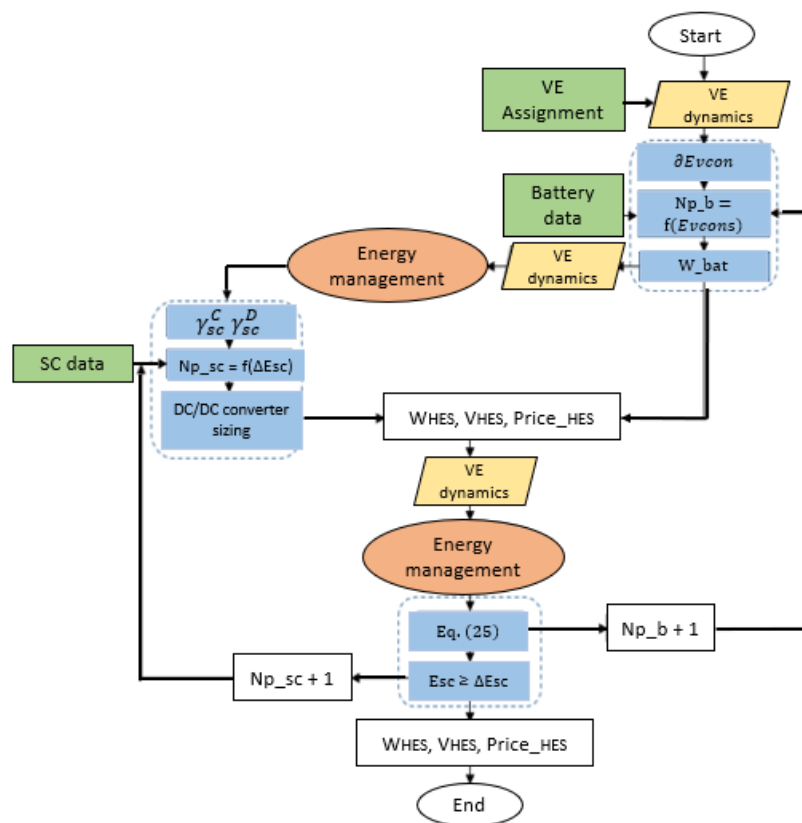


Figure 5. HESS sizing algorithm schematic [37].

4. Results

4.1. Requested Power and Energy

Following Section 3, a sizing algorithm was implemented on the Matlab/Simulink software environment. Figure 6 shows the power profile of 80 s of VDI drive cycle detailed in Section 2. A 90% yield was applied on traction and lifting powers to take into account loss from the inverter and the electric motor. According to the forklift datasheet, the motor for lifting operation is sized for a nominal power of 6 kW which matches the power in lowering phases. Equations (4)–(7) are basics and do not take into account all the forces such as resistive forces. In addition, the acceleration time was set arbitrarily short (not given in the datasheet). Moreover, during the VDI drive cycle, the forklift is only handling 70% of the maximum load.

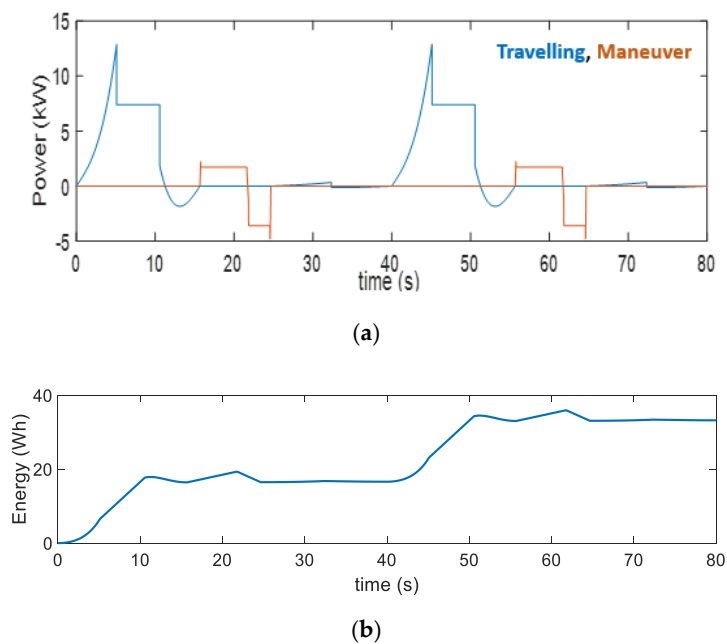


Figure 6. (a) Power and energy requested from the VDI drive cycle—(blue) traction power (red) lifting power, (b) Energy requested from the VDI drive cycle—(blue) total energy from traction and lifting power.

A 4 kW motor is announced for traction operations, whereas simulations show power peaks of up to 12 kW (Figure 6). In fact, assumptions were made, when the VDI drive cycle was built, as the forklift is travelling at maximal speed with a 70% load, which is not always realistic. Therefore, this hypothesis oversizes the power requested from the forklift and will be taken into account in the final discussion.

4.2. Comparison of Single Source Sizing

Simulations were made to size the forklift for 1, 5, 7, 10 and 12 h of VDI drive cycle for a single energy source. High-power (HP) lithium-ion batteries (Kokam 3.7 V/40 Ah SLPB100216216H, Kokam 3.7 V/75 Ah SLPB125255255H, Winston 3.2 V/40 Ah LFP040AHA) and high-energy lithium-ion batteries (Kokam 3.7 V/40 Ah SLPB90216216, Kokam 3.7 V/75 Ah SLPB120255255, European Battery 3.2 V/45 Ah EB45AH) were used in this study. The results can be found in Figure 7 and Table 3.

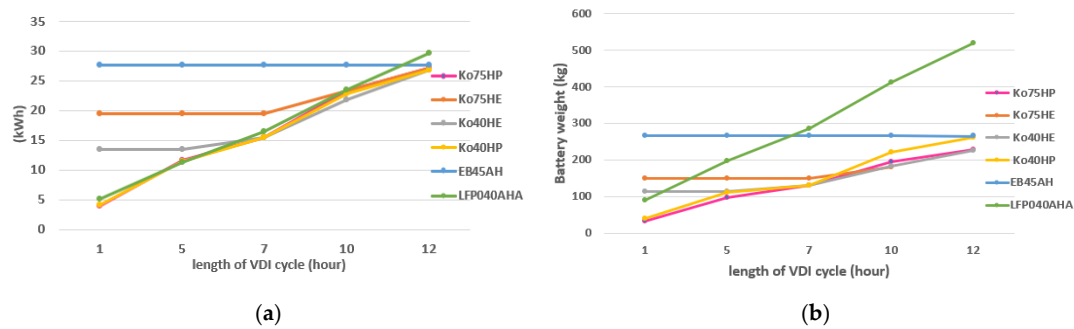


Figure 7. (a) Kilowatt hour per battery pack found after repeating VDI cycle. (b) Battery weight per battery per VDI cycle.

Table 3. Number of cells and capacity for each battery and VDI cycle range.

	VDI Cycle (1 h)			VDI Cycle (5 h)			VDI Cycle (7 h)			VDI Cycle (10 h)			VDI Cycle (12 h)		
	Nsb	Npb	Ah	Nsb	Npb	Ah	Nsb	Npb	Ah	Nsb	Npb	Ah	Nsb	Npb	Ah
Ko75HP	7	2	150	7	6	450	7	8	600	7	12	900	7	14	1050
Ko75HE	7	10	750	7	10	750	7	10	750	7	12	900	7	14	1050
Ko40HE	7	13	520	7	13	520	7	15	600	7	21	840	7	26	1040
Ko40HP	7	4	160	7	11	440	7	15	600	7	22	880	7	26	1040
EB45AH	8	24	1080	8	24	1080	8	24	1080	8	24	1080	8	24	1080
LFP040AHA	8	5	200	8	11	640	8	16	640	8	23	920	8	29	1160

The typical EFG 110 Jungheinrich energy storage system is a 24 V/500 Ah lead-acid battery composed of 12 cells of 2 V/500 Ah connected in series. This information is deduced from the datasheet and the DIN 43,535 A norm. For each lithium-ion battery technology and each operating hour, the total battery weight is always lower than 300 kg, except for LFP040AHA cells, whereas initial lead-acid battery weight is equal to 380 kg (see Figure 7). In addition to the small weight, lithium-ion battery offers better capacity, which is explained by its higher specific energy (Table 2) [24]. One comment can be given on high-power and high-energy battery. Single source sizing was made to provide maximal power traction, maximal power in recovery phase and maximal range for a given operating time [31]. Thus, for lower range (1 h), maximal power is the main criterion to be fulfilled, but high energy is more constraining when the range becomes higher (12 h). Therefore, Figure 7 and Table 2 show that HP batteries are more suitable for a lower range, with fewer cells than HE batteries, which are oversized. However, a 12 h range is already a very high range for forklift application and Figure 7 shows that for different technologies, high power and high energy battery can have the same weight for a specific range. However, for forklift applications, high power batteries are more suitable because of power peaks that must be provided to assure good dynamics.

4.3. Comparison of Hybrid Source

For reasons mentioned in Section 3.2, a HE battery can be used in forklift applications if it is used with a high specific power storage component. Thereby, supercapacitors are able to provide high power peaks in a short amount of time. For this simulation, Maxwell BCAP0350 350 F/2.7 V (sc1), Maxwell BCAP0450 P270 S18 450 F/2.7 V (sc2) and Maxwell BCAP3400 P300 K04/05 3400 F/3.0 V (sc3) supercapacitors were used. Each supercapacitor technology was tested with each of the HE batteries for a 7 h operating time with the VDI drive cycle (Figure 8 and Table 4).

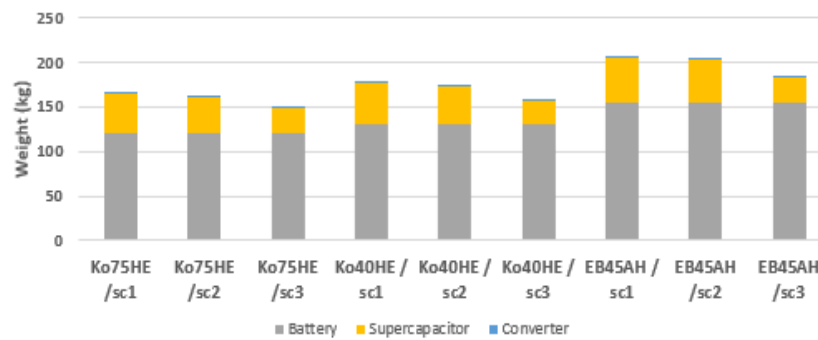


Figure 8. Weight results for the hybrid sizing (7 h VDI cycle range).

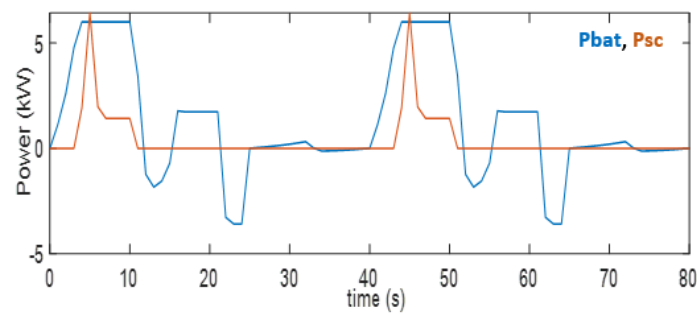
Table 4. Results from hybridization (number of cells, capacity and volume).

	VDI Cycle (7 h)									
	Battery					Supercapacitor			Converter	
	Nsb	Npb	Ah	kWh	Vol	Ns_sc	Np_sc	kWh	Vol	Vol
Ko75HE/sc1	7	8	600	15.5	65.7	9	57	0.1	38	0.18
Ko75HE/sc2	7	8	600	15.5	65.7	9	44	0.1	33.8	0.18
Ko75HE/sc3	7	8	600	15.5	65.7	8	5	0.1	27.7	0.18
Ko40HE/sc1	7	15	600	15.5	64.8	9	58	0.1	3.87	0.19
Ko40HE/sc2	7	15	600	15.5	64.8	9	45	0.1	34.6	0.19
Ko40HE/sc3	7	15	600	15.5	64.8	8	5	0.1	27.7	0.18
EB45AH/sc1	8	14	630	16.1	92.5	9	64	0.1	42.7	0.19
EB45AH/sc2	8	14	630	16.1	92.5	9	50	0.1	38.5	0.19
EB45AH/sc3	8	14	630	16.1	92.5	8	5	0.1	27.7	0.18

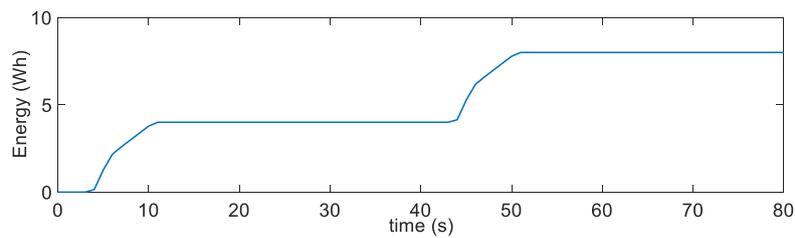
In regard to Figure 8 and Table 3, batteries are sized according to the energy requested, which explains why batteries have approximatively the same energy (kWh). Only 0.1 kWh of supercapacitor must be added to take into account the dynamics of the forklift. If the right set of battery/supercapacitor is found, the weight of the hybrid storage system can be equal to a single source solution (for example, Ko75HE and BCAP3400 (sc3)). Maxwell BCAP3400 SC significantly decreases the weight of the supercapacitor banks because of the nominal voltage of 3 V, which is not common in typical supercapacitors (usually around 2.7 V).

4.4. Energy Management Influence

As the weight is not an issue in forklift application, using lithium-ion batteries enable increasing the vehicle range from 7 h to half a day without reaching the battery weight recommended by the manufacturer. In regard to battery and supercapacitor technologies, the total weight can become lower or higher than a single source solution [39]. In either way, adding a supercapacitor limits battery stresses and improves battery lifetime. It is then critical that SCs act like buffers. The goal of the energy management is to ensure supercapacitor energy to track a reference value in order to be ready to provide or store energy from any operational phases. The power battery limitation detailed in Section 3.3 is then illustrated in Figures 9 and 10. Power battery limitations P_{batD} and P_{batC} were set at 6 and -6 kW. Without violating those limitations, battery or load power is used to recharge supercapacitors to prevent them from any energy drift (Figure 9b).

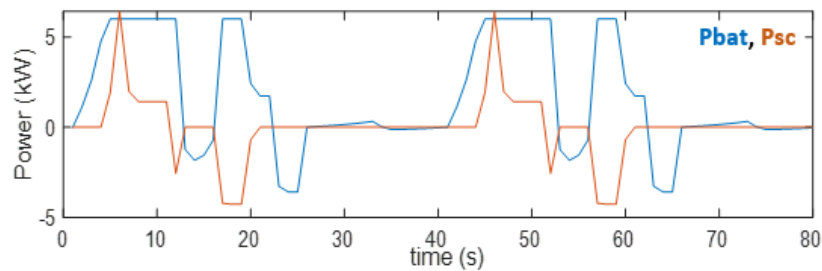


(a)

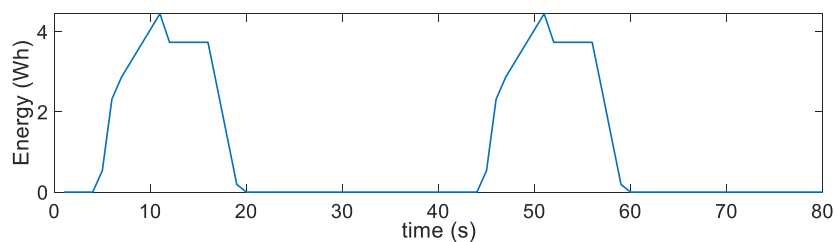


(b)

Figure 9. (a) Battery power limitation without supercapacitor energy supervision (battery power in blue, supercapacitor power in red). (b) Supercapacitor energy.



(a)



(b)

Figure 10. (a) Battery power limitation with supercapacitor energy supervision (battery power in blue, supercapacitor power in red). (b) Supercapacitor energy.

Simulations were made to emphasize the importance of energy management. Figure 11 shows weight results for a hybrid sizing with the EB45AH and BCAP0350 and a 7 h operation. The power split algorithm is ruled by the power limitation chosen. Usually, they are chosen according to the manufacturer specifications. For previous simulations, they were chosen arbitrarily as 8 to -8 kW (Figure 8 and Table 3). Different values of power battery limitations were set. The results show that, for

this energy management strategy, the smaller the battery power limits are, the higher the supercapacitor weight is and therefore higher the overall HESS weight is (Figure 11 and Table 5).

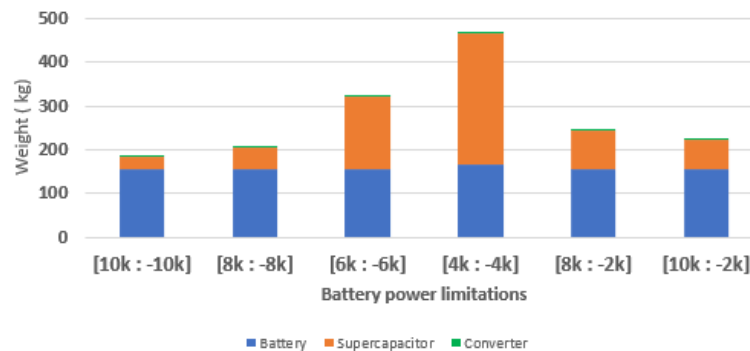


Figure 11. Weight results according to different power battery limits.

Table 5. Results from energy management test (number of cells, capacity and volume).

	EB45AH/BCAP0350—VDI Cycle (7 h)									
	Battery					Supercapacitor			Converter	
	Nsb	Npb	Ah	kWh	Vol	Ns_sc	Np_sc	kWh	Vol	Vol
[10 k:−10 k]	8	14	630	16.13	92.49	9	34	0.069	22.7	0.1
[8 k:−8 k]	8	14	630	16.13	92.49	9	64	0.13	42.73	0.19
[6 k:−6 k]	8	14	630	16.13	92.49	9	209	0.425	139.5	0.36
[4 k:−4 k]	8	14	675	17.28	99.1	9	376	0.764	251.1	0.53
[8 k:−2 k]	8	14	630	16.13	92.49	9	113	0.23	75.46	0.25
[10 k:−2 k]	8	14	630	16.13	92.19	9	83	0.169	55.42	0.15

4.5. Price Constraint

As shown in previous results, the weight of the forklift energy storage system can be drastically decreased using a Li-ion battery instead of a lead-acid battery. In forklift applications, weight is not an issue and it is better if the battery is quite heavy. Therefore, a lot of battery cells can be added to increase the vehicle range (hours of operations) until meeting the forklift battery weight specification.

The only limit is then the price. Lithium-ion batteries display an average cost of 176 USD/kWh in 2018 [54] against 150 USD/kWh for lead-acid battery [55]. Nevertheless, Li-ion battery cost is still decreasing, and they request less maintenance and last much longer [54]. Therefore, it can be assumed that the total cost of ownership [19] of a lithium-ion forklift is better than a classical electric forklift. Moreover, by adding an extra USD/kWh of a supercapacitor and some more for the converter [39] the ageing of the battery is improved and allows the forklift to be more efficient and to last longer.

4.6. Ageing Analysis

In fact, our model does not take into account the ageing of the battery. However, RMS power provided by the battery can be analyzed. If the bus voltage is supposed to be almost constant during operation, therefore the power profile will be almost the same as the current profile. The higher the current, the higher the heat loss that will occur in the internal resistance of the battery. However, heat is one of the critical ageing factors [11,21,22,56,57]. Therefore, by decreasing the RMS battery power, battery lifetime can be improved. Simulations (Figure 12) were made for a single source and for a hybrid source to fulfill a 7 h VDI cycle. Power battery limitations were also changed from [8, −8 kW] to [6, −6 kW]. The results show that HESS decreases RMS battery power from 3% to 10% following the case study. In fact, with additional supercapacitor, battery power stresses can be decreased even more (example of [6, −6 kW] battery power limitations in Figure 12). Therefore, with a HESS, battery ageing is reduced. The use of optimal energy management is crucial to limit battery stresses.

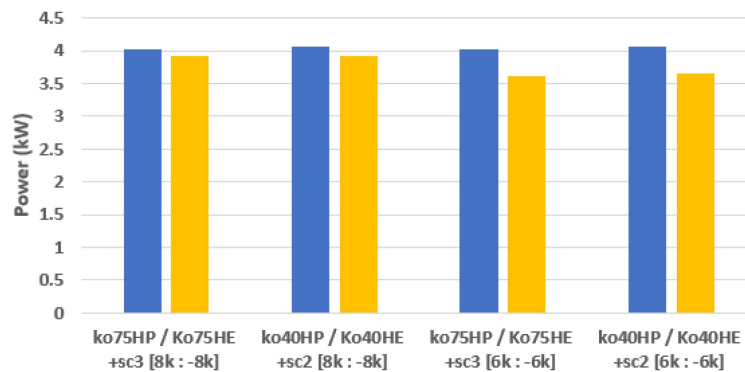


Figure 12. RMS battery power for a single source (blue) and a HESS (yellow).

5. Conclusions

The sizing of a hybrid energy storage system using a lithium-ion battery and a supercapacitor for a forklift application has been presented in this study. Unlike automotive applications, where the weight of the battery is designed to be as light as possible, the weight of the overall forklift must be high enough to allow the counterbalance effect during lifting operations. Simulations show that even for a very high range of operation (12 h) and an oversized requested power, the HESS is still lighter than the lead-acid battery recommended by the manufacturer, in regard to battery and supercapacitor cells chosen. Despite a higher price compared to the lead-acid battery, lithium-ion technology has better power performance, energy efficiency, cycle life, charging time and needs less maintenance. Moreover, supercapacitors allow for a better yield in regard to recovery power during braking and lowering phases, and allow one to put less stress on the battery. In fact, thanks to the energy management presented, RMS battery power can be reduced down to 10%, compared to a single source solution, and therefore improve the battery ageing. An optimal energy management algorithm is absolutely critical to improve battery lifetime. Finally, with hybridization, the forklift battery total cost of ownership is also improved compared to the current solution with lead-acid batteries. Light weight issues can be solved by adding extra ballast to meet battery weight specifications.

Author Contributions: Supervision, T.M. and W.U.; Writing—original draft, T.P.; Writing—review & editing, T.M., S.D. and D.F. All authors have read and agreed to the published version of the manuscript.

Funding: This research was funded in part by the "Programme INTERREG V A Rhin Supérieur: Dépasser les frontières, projet après projet", with FEDER: Fonds Européen de Développement Régional.

Acknowledgments: The authors would like to thank Estelle Fischer for her contribution in the context of a technological project at INSA Strasbourg.

Conflicts of Interest: The authors declare no conflict of interest.

Nomenclature

Variable	Description
F_{aero}	Resistive force due to aerodynamic
F_{wheel}	Resistive force due to wheels
F_{gx}, F_g	Resistive forces due to gravity
F_T	Traction force
F_{lift}	Lifting (and lowering) force due to the fork
V_{VEH}	Longitudinal vehicle velocity
V_{fork}	Longitudinal fork velocity
m_{fkt}	Forklift mass
m_{load}	Load mass
P_v	Power from travelling operation

P_{lift}	Power from lifting operation
U_{bus}	Bus voltage
N_{sb}	Number of battery cells in series
N_{pb}	Number of battery cells in parallel
U_{elb}	Nominal voltage of one battery cell
$E_{v_{cons}}$	Energy requested by the vehicle ($P_v + P_{lift}$)
E_{elB}	Energy of one battery cell
M_{elB}	Mass of one battery cell
R_{0elb}	Internal resistance of the battery
DOD	Depth of discharge
$\partial E_{v_{cons}}$	Gradient of energy requested over mass
N_{psc}	Number of supercapacitor cells in series
N_{psc}	Number of supercapacitor cells in parallel
$U_{el_{sc}}$	Nominal voltage of one supercapacitor cell
$M_{el_{sc}}$	Mass of one supercapacitor cell
$C_{el_{sc}}$	Capacity of one supercapacitor cell
ΔE_{sc}	Maximum variation of supercapacitor energy
γ_{sc}^C	Gradient of maximum supercapacitor energy requested over mass
γ_{sc}^D	Gradient of minimum supercapacitor energy requested over mass

References

- Brettel, M.; Friederichsen, N.; Keller, M.; Rosenberg, M. How Virtualization, Decentralization and Network Building Change the Manufacturing Landscape: An Industry 4.0 Perspective. *Int. J. Mech. Aerosp. Ind. Mechatron. Manuf. Eng.* **2014**, *8*, 37–44.
- Lee, J.; Bagheri, B.; Kao, H.A. A Cyber-Physical Systems architecture for Industry 4.0-based manufacturing systems. *Manuf. Lett.* **2015**, *3*, 18–23. [[CrossRef](#)]
- Lasi, H.; Kemper, H.-G.; Fetteke, P.; Thomas, F.; Hoffman, M. *Industry 4.0*; no. Business & Information Systems Engineering; Springer Fachmedien Wiesbad: Wiesbaden, Germany, 2014; Volume 2014.
- Rüßmann, M.; Lorenz, M.; Gerbert, P.; Waldner, M.; Justus, J.; Engel, P.; Harnish, M. *Industry 4.0 The Future of Productivity and Growth in Manufacturing Industries*; The Boston Consulting Group: Boston, MA, USA, 2015.
- Lom, M.; Pribyl, O.; Svitek, M. Industry 4.0 as a part of smart cities. In Proceedings of the 2016 Smart Cities Symposium Prague, SCSP 2016, Prague, Czech Republic, 26–27 May 2016.
- Cao, L.; Depner, T.; Borstell, H.; Richter, K. Discussions on sensor-based assistance systems for forklifts. In Proceedings of the Smart SysTech 2019—European Conference on Smart Objects, Systems and Technologies, Magdeburg, Germany, 4–5 June 2019; pp. 35–42.
- Mohammadi, A.; Mareels, I.; Oetomo, D. Model predictive motion control of autonomous forklift vehicles with dynamics balance constraint. In Proceedings of the 2016 14th International Conference on Control, Automation, Robotics and Vision, ICARCV 2016, Phuket, Thailand, 13–15 November 2016; Volume 2016, pp. 13–15.
- Kim, S.; Choi, S.; Lee, J.; Hong, S.; Yoon, J. A study of hybrid propulsion system on forklift trucks. In Proceedings of the 2013 World Electric Vehicle Symposium and Exhibition, EVS 2014, Barcelona, Spain, 17–20 November 2013; pp. 1–8.
- Fuc, P.; Kurczewski, P.; Lewandowska, A.; Nowak, E.; Selech, J.; Ziolkowski, A. An environmental life cycle assessment of forklift operation: A well-to-wheel analysis. *Int. J. Life Cycle Assess.* **2016**, *21*, 1438–1451. [[CrossRef](#)]
- Li, J.; Lutzemberger, G.; Poli, D.; Scarpelli, C.; Piazza, T. Simulation and experimental validation of a hybrid forklift truck. In Proceedings of the 2019 AEIT International Conference of Electrical and Electronic Technologies for Automotive (AEIT AUTOMOTIVE), Torino, Italy, 2–4 July 2019.
- Dezza, F.C.; Musolino, V.; Piegari, L.; Rizzo, R. Hybrid battery-supercapacitor system for full electric forklifts. *IET Electr. Syst. Transp.* **2019**, *9*, 16–23. [[CrossRef](#)]
- Lototsky, M.V.; Tolj, I.; Parsons, A.; Smith, F.; Sita, C.; Linkov, V. Performance of electric forklift with low-temperature polymer exchange membrane fuel cell power module and metal hydride hydrogen storage extension tank. *J. Power Sources* **2016**, *316*, 239–250. [[CrossRef](#)]

13. Schaltz, E.; Khaligh, A.; Rasmussen, P.O. Influence of battery/ultracapacitor energy-storage sizing on battery lifetime in a fuel cell hybrid electric vehicle. *IEEE Trans. Veh. Technol.* **2009**, *58*, 3882–3891. [[CrossRef](#)]
14. Kim, T.H.; Lee, S.J.; Choi, W. Design and control of the phase shift full bridge converter for the on-board battery charger of the electric forklift. In Proceedings of the 8th International Conference of Power Electronics—ECCE Asia “Green World with Power Electronics ICPE 2011-ECCE Asia, Jeju, Korea, 30 May–3 June 2011; pp. 2709–2716.
15. Khaligh, A.; Li, Z. Battery, ultracapacitor, fuel cell, and hybrid energy storage systems for electric, hybrid electric, fuel cell, and plug-in hybrid electric vehicles: State of the art. *IEEE Trans. Veh. Technol.* **2010**, *59*, 2806–2814. [[CrossRef](#)]
16. Battery Reality: There’s Nothing Better Than Lithium-Ion Coming Soon—Bloomberg. Available online: <https://www.bloomberg.com/news/articles/2019-04-03/battery-reality-there-s-nothing-better-than-lithium-ion-coming-soon> (accessed on 15 January 2020).
17. Hannan, M.A.; Member, S. State-of-the-Art and Energy Management System of Lithium-Ion Batteries in Electric Vehicle Applications: Issues and Recommendations. *IEEE Access* **2018**, *6*, 19362–19378. [[CrossRef](#)]
18. Amrouche, S.O.; Rekioua, D.; Rekioua, T.; Bacha, S. Overview of energy storage in renewable energy systems. *Int. J. Hydrog. Energy* **2016**, *41*, 20914–20927. [[CrossRef](#)]
19. Babin, A.; Rizoug, N.; Mesbahi, T.; Boscher, D.; Hamdoun, Z. Total Cost of Ownership Improvement of Commercial Electric Vehicles Using Battery Sizing and Intelligent Charge Method. *IEEE Trans. Ind. Appl.* **2018**, *54*, 1691–1700. [[CrossRef](#)]
20. Kuperman, A.; Aharon, I. Battery-ultracapacitor hybrids for pulsed current loads: A review. *Renew. Sustain. Energy Rev.* **2011**, *15*, 981–992. [[CrossRef](#)]
21. Fleischhammer, M.; Waldmann, T.; Bisle, G.; Hogg, B.I.; Wohlfahrt-Mehrens, M. Interaction of cyclic ageing at high-rate and low temperatures and safety in lithium-ion batteries. *J. Power Sources* **2015**, *274*, 432–439. [[CrossRef](#)]
22. Cao, J.; Emadi, A. A New Battery/Ultra-Capacitor Hybrid Energy Storage System for Electric, Hybrid and Plug-in Hybrid Electric Vehicles. In Proceedings of the 2009 IEEE Vehicle Power and Propulsion Conference, Dearborn, MI, USA, 7–9 September 2009; pp. 941–946.
23. Sadoun, R.; Rizoug, N.; Bartholomeus, P.; Le Moigne, P. Optimal architecture of the hybrid source (battery/supercapacitor) supplying an electric vehicle according to the required autonomy. In Proceedings of the 2013 15th Europe Conference on Power Electronics and Applications EPE 2013, Lille, France, 2–6 September 2013.
24. Mesbahi, T.; Rizoug, N.; Bartholomeüs, P.; Sadoun, R.; Khenfri, F.; le Moigne, P. Optimal Energy Management for a Li-Ion Battery/Supercapacitor Hybrid Energy Storage System Based on a Particle Swarm Optimization Incorporating Nelder Mead Simplex Approach. *IEEE Trans. Intell. Veh.* **2017**, *2*, 99–110. [[CrossRef](#)]
25. Herrera, V.; Milo, A.; Gaztañaga, H.; Etxeberria-otadui, I.; Villarreal, I. Adaptive energy management strategy and optimal sizing applied on a battery-supercapacitor based tramway. *Appl. Energy* **2016**, *169*, 831–845. [[CrossRef](#)]
26. Joshi, M.C.; Samanta, S.; Srungavarapu, G. Frequency Sharing Based Control of Battery/Ultracapacitor Hybrid Energy System in the Presence of Delay. *IEEE Trans. Veh. Technol.* **2019**, *68*, 10571–10584. [[CrossRef](#)]
27. Khalid, M. A Review on the Selected Applications of Battery-Supercapacitor Hybrid Energy Storage Systems for Microgrids. *Energies* **2019**, *12*, 4559. [[CrossRef](#)]
28. Douglas, H.; Pillay, P. Sizing ultracapacitors for hybrid electric vehicles. In Proceedings of the IECON Proc. (Industrial Electronics Conference 2005), Raleigh, NC, USA, 6–10 November 2005; Volume 2005, pp. 1599–1604.
29. Vadlamudi, S.D.V.R.; Kumtepel, V.; Ozcira, S.; Tripathi, A. Hybrid energy storage power allocation and motor control for electric forklifts. In Proceedings of the 2016 Asian Conference Energy, Power and Transportation Electrification (ACEPT) 2016, Singapore, 25–27 October 2016; pp. 1–5.
30. Ostadi, A.; Kazerani, M. A Comparative Analysis of Optimal Sizing of Battery-Only, Ultracapacitor-Only, and Battery-Ultracapacitor Hybrid Energy Storage Systems for a City Bus. *IEEE Trans. Veh. Technol.* **2015**, *64*, 4449–4460. [[CrossRef](#)]
31. Meyer, R.T.; Decarlo, R.A.; Pekarek, S. Hybrid model predictive power management of a battery-supercapacitor electric vehicle. *Asian J. Control* **2016**, *18*, 150–165. [[CrossRef](#)]

32. Stroe, D.; Swierczynski, M. Accelerated Aging of Lithium-Ion Batteries based on Electric Vehicle Mission Profile. In Proceedings of the 2017 IEEE Energy Conversion Congress and Exposition (ECCE), Cincinnati, OH, USA, 1–5 October 2017; pp. 5631–5637.
33. Feroldi, D.; Zumoffen, D. Sizing methodology for hybrid systems based on multiple renewable power sources integrated to the energy management strategy. *Int. J. Hydrog. Energy* **2014**, *39*, 8609–8620. [[CrossRef](#)]
34. Araújo, R.E.; de Castro, R.; Pinto, C.; Melo, P.; Freitas, D. Combined sizing and energy management in EVs with batteries and supercapacitors. *IEEE Trans. Veh. Technol.* **2014**, *63*, 3062–3076. [[CrossRef](#)]
35. Sampietro, J.L.; Puig, V.; Costa-Castelló, R. Optimal Sizing of Storage Elements for a Vehicle Based on Fuel Cells, Supercapacitors, and Batteries. *Energies* **2019**, *12*, 925. [[CrossRef](#)]
36. Wang, Y.; Yang, Z.; Li, F.; An, X.; Lin, F. Optimization of Energy Management Strategy and Sizing in Hybrid Storage System for Tram. *Energies* **2018**, *11*, 752. [[CrossRef](#)]
37. Paul, T.; Mesbahi, T.; Durand, S.; Flieller, D.; Uhring, W. Study and Influence of Standardized Driving Cycles on the Sizing of Li-Ion Battery/Supercapacitor Hybrid Energy Storage. In Proceedings of the 2019 IEEE Vehicle Power and Propulsion Conference (VPPC), Dearborn, MI, USA, 7–9 September 2019; pp. 1–6.
38. Hammani, A.; Sadoun, R.; Rizoug, N.; Bartholomeüs, P.; Barbedette, B.; le Moigne, P. Influence of the management strategies on the sizing of hybrid supply composed with battery and supercapacitor. In Proceedings of the 2012 1st International Conference on Renewable Energies and Vehicular Technology (RENET 2012), Nabeul, Tunisia, 26–28 March 2012; pp. 1–7.
39. Sadoun, R.; Rizoug, N.; Bartholomeüs, P.; Barbedette, B.; Lemoigne, P. Sizing of hybrid supply (battery-supercapacitor) for electric vehicle taking into account the weight of the additional Buck-Boost chopper. In Proceedings of the 2012 1st International Conference on Renewable Energies and Vehicular Technology (RENET 2012), Nabeul, Tunisia, 26–28 March 2012; pp. 8–14.
40. Mahayadin, A.R.; Ibrahim, I. Development of Driving Cycle Construction Methodology in Malaysia's Urban Road System. In Proceedings of the 2018 International Conference Computational Approach in Smart Systems Design and Applications (ICASSDA), Kuching, Malaysia, 15–17 August 2018; pp. 1–5.
41. Hosseinzadeh, E.; Rokni, M.; Advani, S.G.; Prasad, A.K. Performance simulation and analysis of a fuel cell/battery hybrid forklift truck. *Int. J. Hydrog. Energy* **2013**, *38*, 4241–4249. [[CrossRef](#)]
42. Omar, N.; Monem, M.A.; Firouz, Y.; Salminen, J.; Smekens, J.; Hegazy, O.; Gaulous, H.; Mulder, G.; Bossche, P.V.D.; Coosemans, T.; et al. Lithium iron phosphate based battery—Assessment of the aging parameters and development of cycle life model. *Appl. Energy* **2014**, *113*, 1575–1585. [[CrossRef](#)]
43. Sadoun, R.; Rizoug, N.; Bartholomeüs, P.; Barbedette, B.; le Moigne, P. Optimal sizing of hybrid supply for electric vehicle using Li-ion battery and supercapacitor. In Proceedings of the 2011 IEEE Vehicle Power and Propulsion Conference, VPPC 2011, Chicago, IL, USA, 5–8 September 2011.
44. Song, Z.; Hofmann, H.; Li, J.; Hou, J.; Han, X.; Ouyang, M. Energy management strategies comparison for electric vehicles with hybrid energy storage system. *Appl. Energy* **2014**, *134*, 321–331. [[CrossRef](#)]
45. Zheng, C.; Li, W.; Liang, Q. An Energy Management Strategy of Hybrid Energy Storage Systems for Electric Vehicle Applications. *IEEE Trans. Sustain. Energy* **2018**, *9*, 1880–1888. [[CrossRef](#)]
46. Castaings, A.; Lhomme, W.; Trigui, R.; Bouscayrol, A. Comparison of energy management strategies of a battery/supercapacitors system for electric vehicle under real-time constraints. *Appl. Energy* **2016**, *163*, 190–200. [[CrossRef](#)]
47. Wirasingha, S.G.; Emadi, A. Classification and review of control strategies for plug-in hybrid electric vehicles. *IEEE Trans. Veh. Technol.* **2011**, *60*, 111–122. [[CrossRef](#)]
48. Sun, L.; Feng, K.; Chapman, C.; Zhang, N. An adaptive power-split strategy for battery-supercapacitor powertrain-design, simulation, and experiment. *IEEE Trans. Power Electron.* **2017**, *32*, 9364–9375. [[CrossRef](#)]
49. Long, B.; Lim, S.T.; Bai, Z.F.; Ryu, J.H.; Chong, K.T. Energy Management and Control of Electric Vehicles, Using Hybrid Power Source in Regenerative Braking Operation. *Energies* **2014**, *7*, 4300–4315. [[CrossRef](#)]
50. Paul, T.; Mesbahi, T.; Durand, S.; Flieller, D.; Uhring, W. Smart Energy management of Li-ion battery/Supercapacitor Hybrid Energy Storage System for Electric Vehicle Application. In Proceedings of the PCIM EUROPE, Nuremberg, Germany, 7–9 May 2019; pp. 7–9.
51. Mesbahi, T.; Khenfri, F.; Rizoug, N.; Bartholome, P.; le Moigne, P. Combined Optimal Sizing and Control of Li-Ion Battery/Supercapacitor Embedded Power Supply Using Hybrid Particle Swarm—Nelder—Mead Algorithm. *IEEE Trans. Sustain. Energy* **2017**, *8*, 59–73. [[CrossRef](#)]

52. González, A.; Goikolea, E.; Barrena, J.A.; Mysyk, R. Review on supercapacitors: Technologies and materials. *Renew. Sustain. Energy Rev.* **2016**, *58*, 1189–1206. [[CrossRef](#)]
53. Rizoug, N.; Sadoun, R.; Mesbahi, T.; Bartholomeus, P.; Lemoigne, P. Aging of high power Li-ion cells during real use of electric vehicles. *IET Electr. Syst. Transp.* **2017**, *7*, 14–22. [[CrossRef](#)]
54. A Behind the Scenes Take on Lithium-ion Battery Prices. BloombergNEF. Available online: <https://about.bnef.com/blog/behind-scenes-take-lithium-ion-battery-prices/> (accessed on 17 January 2020).
55. Lead-Acid Batteries Are on a Path to Extinction. Available online: <https://www.forbes.com/sites/rrapier/2019/10/13/lead-acid-batteries-are-on-a-path-to-extinction/> (accessed on 17 January 2020).
56. Rajani, S.V.; Pandya, V.J. Ultracapacitor-battery hybrid energy storage for pulsed, cyclic and intermittent loads. In Proceedings of the 2016 IEEE 6th International Conference on Power Systems ICPS 2016, New Delhi, India, 4–6 March 2016; pp. 1–6.
57. Li, W.; Joós, G. A power electronic interface for a battery supercapacitor hybrid energy storage system for wind applications. In Proceedings of the PESC Rec.—IEEE Annual Power Electronics Specialists Conference, Rhodes, Greece, 15–19 June 2008; pp. 1762–1768.



© 2020 by the authors. Licensee MDPI, Basel, Switzerland. This article is an open access article distributed under the terms and conditions of the Creative Commons Attribution (CC BY) license (<http://creativecommons.org/licenses/by/4.0/>).